

# Quantifying Ocular Surface Inflammation and Correlating It With Inflammatory Cell Infiltration In Vivo: A Novel Method

Giulio Ferrari,<sup>1</sup> Alessandro Rabiolo,<sup>1</sup> Fabio Bignami,<sup>1</sup> Federico Sizzano,<sup>\*,2,3</sup> Alessio Palini,<sup>\*,2,3</sup> Chiara Villa,<sup>3</sup> and Paolo Rama<sup>1</sup>

<sup>1</sup>Cornea and Ocular Surface Disease Unit, Eye Repair Lab, IRCCS San Raffaele Scientific Institute, Milan, Italy

<sup>2</sup>Flow Cytometry Resource Advanced Cytometry Technical Applications Laboratory, IRCCS San Raffaele Scientific Institute, Milan, Italy

<sup>3</sup>Flow Cytometry Core Facility, Nestlé Institute of Health Sciences, Lausanne, Switzerland

Correspondence: Giulio Ferrari, Cornea and Ocular Surface Disease Unit, Eye Repair Lab, IRCCS San Raffaele Scientific Institute, Via Olgettina 60, 20132 Milan, Italy; ferrari.giulio@hsr.it.

Current affiliation: \*Nestlé Institute of Health Sciences, Lausanne, Switzerland.

Submitted: April 15, 2015

Accepted: September 15, 2015

Citation: Ferrari G, Rabiolo A, Bignami F, et al. Quantifying ocular surface inflammation and correlating it with inflammatory cell infiltration in vivo: a novel method. *Invest Ophthalmol Vis Sci.* 2015;56:7067-7075. DOI:10.1167/iovs.15-17105

**PURPOSE.** The purpose of this study was to develop a novel, objective, and semiautomated method to quantify conjunctival redness by correlating measured redness with standard clinical redness and symptom scales and inflammatory cell infiltration.

**METHODS.** Eleven outpatients presenting with mild to severe conjunctival hyperemia were included in the study. Clinical examination included patient history; visual analogue score (VAS) for ocular symptoms; 25-item National Eye Institute Visual Function Questionnaire (NEI-VFQ 25) for quality of life/vision; photographs of the anterior segment graded for conjunctival hyperemia, using Efron, relative redness of image (RRI), and edge feature (EF) scales; and conjunctival impression cytology analyzed by flow cytometry. Differences between affected and unaffected eyes were evaluated, and correlations among questionnaire scores, ocular hyperemia grading scores, and assessment of biological markers were performed.

**RESULTS.** Visual analogue score ( $P < 0.0001$ ), Efron scale ( $P = 0.0003$ ), RRI scores ( $P = 0.0004$ ), and EF scores ( $P < 0.0001$ ) and the percentage of granulocytes (defined as cluster of differentiation [CD] 45<sup>dim</sup>;  $P = 0.0080$ ) were significantly higher in affected eyes. Conversely, the percentage of CD45<sup>bright</sup> leukocytes was reduced in affected eyes ( $P = 0.0054$ ). Both the RRIs and EFs were positively correlated with VAS, Efron scale, percentages of conjunctival granulocytes, and CD45<sup>bright</sup>CD3<sup>neg</sup> cells, whereas they were negatively correlated with the percentage of CD45<sup>bright</sup>CD3<sup>pos</sup> cells. Edge feature and RRI were correlated (Spearman  $r = 0.78$ ,  $P < 0.0001$ ).

**CONCLUSIONS.** Ocular redness is a cardinal sign driving clinical judgment in highly prevalent ocular disorders; hence, we suggest that our semiautomated and reproducible method may represent a helpful tool in the follow-up of these patients.

**Keywords:** conjunctival hyperemia, grading score, image processing, impression cytology, ocular redness

**SCOPO.** Sviluppare un nuovo metodo quantitativo e semiautomatico per quantificare l'iperemia congiuntivale e correlarla con parametri clinici e biologici.

**METODI.** Undici pazienti ambulatoriali con iperemia congiuntivale da lieve a severa sono stati inclusi nello studio. I pazienti arruolati sono stati valutati al basale e  $20 \pm 8$  giorni dopo. L'esame clinico includeva: storia del paziente; questionario Visual Analogue Score (VAS) al fine di valutare la sintomatologia oculare; questionario 25-Item National Eye Institute Visual Function Questionnaire (NEI-VFQ 25) al fine di valutare la qualità della vita e della visione; fotografie del segmento anteriore analizzate con scala di Efron, Relative Redness of Image (RRI) e Edge Feature (EF); citologia ad impressione congiuntivale processata tramite citometria a flusso. Sono state indagate le differenze tra occhi affetti e non-affetti e le correlazioni tra punteggi ottenuti ai questionari, grado di iperemia congiuntivale e parametri biologici.

**RISULTATI.** Le seguenti misure: VAS ( $P < 0.0001$ ), scala di Efron ( $P = 0.0003$ ), RRI ( $P = 0.0004$ ), EF ( $P < 0.0001$ ), e la percentuale di granulociti (definiti come CD45<sup>dim</sup>) ( $P = 0.0080$ ) sono emerse significativamente maggiori negli occhi affetti. Di contro, la percentuale di leucociti CD45<sup>bright</sup> era ridotta negli occhi affetti ( $P = 0.0054$ ). Sia RRI che EF sono risultati positivamente correlati a VAS, scala di Efron, percentuale di granulociti congiuntivali e cellule CD45<sup>bright</sup>CD3<sup>neg</sup>, mentre sono risultati negativamente correlati con la percentuale di cellule CD45<sup>bright</sup>CD3<sup>pos</sup>. EF e RRI hanno mostrato una correlazione reciproca (Spearman  $r = 0.78$ ,  $P < 0.0001$ ).

**CONCLUSIONI.** L'iperemia congiuntivale è un segno cardine d'inflammatione, che guida il giudizio clinico in malattie oculari altamente prevalenti, quindi, suggeriamo che il metodo semiautomatico e riproducibile da noi sviluppato possa rappresentare un utile ausilio nel monitoraggio nel tempo di questi pazienti.

Among the four cardinal signs heralding inflammation (i.e., rubor, tumor, dolor, and calor), rubor (i.e., redness) of the bulbar conjunctiva is the most relevant driver of clinical judgment in cases of ocular surface disorders. Objective and repeatable grading is key in the follow-up of a number of highly prevalent and disabling disorders, including keratitis,<sup>1</sup> uveitis,<sup>2</sup> dry eye,<sup>3</sup> and others.<sup>4</sup> This is particularly relevant in clinical trials, where standardized and consistent endpoint measurements are highly desirable. A number of methods have been proposed to measure conjunctival redness. Among these, we can differentiate between manual qualitative methods, or grading scales, and semi- or fully automatic methods.

In grading scales, a score is arbitrarily given depending on the number, density, and tortuosity of vessels. The Efron,<sup>5</sup> validated bulbar redness,<sup>6</sup> and McMonnies scales are among the scales most frequently used.<sup>7</sup> Despite their intuitiveness, clinical grading scales exhibit extreme variability among different investigators<sup>8</sup> as well as for the same observer over time.<sup>9</sup>

In order to overcome the limits of qualitative measurements, several (semi-) automated techniques have been described. Most of them are based on a combination of color quantification,<sup>10-13</sup> edge detection,<sup>11</sup> and fractal analysis.<sup>14</sup> Although they quantify conjunctival hyperemia objectively and reproducibly, such methods have not widely spread into clinical practice due to the requirement of dedicated instruments and/or trained operators, setup costs, accessibility, and amount of time needed to analyze images.

To overcome these pitfalls, we developed a method to objectively quantify ocular hyperemia by using instruments commonly found in ophthalmic outpatient clinics (i.e., a slit-lamp unit and a computer) in a simple and low-cost way. The algorithm we propose here quantifies ocular redness by detection of edge feature (EF) and relative color extraction (i.e., relative redness of the image [RRI]). Both of the algorithms assign a number from 0 to 1, to each pixel of the slit-lamp image. A value of zero is assigned to a pixel having "no red," whereas a value of 1 is assigned to a "red" pixel. This method does not require human intervention in the grading, hence, variability is limited to image capture, which can be easily reduced by setting standardized parameters (slit-lamp beam, light intensity, and others). For this reason, it could be easily used in the follow-up of patients, thus reducing interoperator variability and assessment of patient status by different physicians over time.

In order to validate our method, we correlated results with those obtained with manual grading scales (Efron) or questionnaires to assess ocular symptoms (visual analogue score [VAS])<sup>15</sup> and the impact of the disease on quality of vision/life (25-Item National Eye Institute Visual Function Questionnaire [NEI-VFQ 25]).<sup>16,17</sup> In addition, we assessed whether our results correlated with objective signs of inflammation, specifically leukocyte infiltration, measured by flow cytometry performed using conjunctival impression cytology samples.

## METHODS

### Study Population

A total of eleven patients affected by mild to severe conjunctival hyperemia were included in this prospective observational study. Patient characteristics are reported in the

Table. Mean ( $\pm$ SD [standard deviation]) patient age was  $60.0 \pm 14.5$  (range, 35-79) years, and there were six males and five females. The healthy eye of 5 of the 11 subjects served as an internal control (no conjunctival hyperemia). Mean age ( $\pm$ SD) of internal controls was  $60.8 \pm 12.7$  (range, 44-76) years; two were male and three were female. No significant age differences between patients and controls was appreciated ( $P = 0.9172$ ). The study was conducted at the Cornea and Ocular Surface Disease Unit, San Raffaele Hospital, Milan, Italy, in compliance with the Declaration of Helsinki and approved by the local ethical committee. Informed consent was obtained. Inclusion criteria were conjunctival hyperemia  $\geq 2$  according to Efron scale for conjunctival redness<sup>5</sup>; and patient age  $\geq 18$  years old. Exclusion criteria were patient was clinically judged at risk for corneal perforation and patient was unable to give informed consent. Enrolled patients were evaluated at baseline (day 0 [D0]) and  $20 \pm 8$  (range, 7-35) days later (D1). The examination included patient history, questionnaires to assess ocular symptoms and quality of vision/life, photographs of the anterior segment, and conjunctival impression cytology. Both eyes were examined at all time points, even if only one eye fit the inclusion criteria. Two patients (nos. 10 and 11) were lost at follow-up.

### Questionnaires

Two copies of the VAS questionnaire were administered to patients, one for each eye, in order to assess ocular symptoms including foreign body sensation, burning/stinging, itching, pain, stick feeling, blurred vision, and photophobia.<sup>15</sup>

An Italian, validated version of the 25-Item National Eye Institute Visual Function Questionnaire (NEI-VFQ 25) was administered to patients in order to assess the impact of the disease on quality of vision/life.<sup>16,17</sup>

### Photograph Acquisition

Two images were acquired for each eye by the same operator (AR). Patients were asked to look temporally and nasally in order to assess nasal and temporal bulbar conjunctiva. Eyelids were held open to reveal the entire cornea and the maximum amount of bulbar conjunctiva.<sup>10</sup> Slit-lamp parameters were set as follows: white light with application of the diffuser, magnification  $\times 10$ , maximum slit width, angle of slit-lamp arm of  $45^\circ$ , and maximum light intensity at one-half. Room lights were switched on. Photographs were stored through the Phoenix version 2.1 software (OPW, Hodgkin, IL, USA) as JPEG (Joint Photographic Experts Group) images with a resolution of  $1624 \times 1232$  pixels. Conjunctival hyperemia was graded by two methods, a manual semiquantitative method and a semiautomatic quantitative method.

### Manual Grading

Manual grading of the anonymized images was performed by an expert clinician (GF) using the Efron scale for conjunctival redness.<sup>5</sup> The Efron scale consists of five images having progressive degrees of ocular hyperemia. A printed color version of the scale is displayed for evaluation by the clinician with no time limit for each image. All images were manually

TABLE. Demographic Features

Patient	Age	Sex, M/F	Race	Affected Eye(s), R/L	Diagnosis	No. of Samples	Days Between Samples
1	70	F	Caucasian	R	Herpes simplex ulcer with fungal superinfection	2	14
2	58	M	Caucasian	R, L	Cicatritial pemphigoid, glaucoma	2	21
3	60	M	Caucasian	L	Herpes simplex ulcer	2	22
4	72	M	Caucasian	R, L	Cicatritial pemphigoid	2	21
5	35	M	Caucasian	R, L	Alkali burn	2	35
6	44	M	Caucasian	R, L	Stevens-Johnson syndrome	2	21
7	54	F	Caucasian	R	Fungal keratitis	2	27
8	44	F	Caucasian	R	<i>Acanthamoeba</i> keratitis	2	13
9	79	F	Caucasian	R, L	Corneal bacterial ulcer, glaucoma	2	7
10	68	F	Caucasian	R, L	Sjögren syndrome	1	n/a
11	76	M	Caucasian	L	Corneal bacterial ulcer	1	n/a

F, female; L, left; M, male; n/a, not available; R, right.

graded within a single session to control for changes in room illumination and/or monitor brightness and contrast.

### Semiautomatic Grading

All images were processed using ImageJ software (<http://imagej.nih.gov/ij/>; provided in the public domain by the National Institutes of Health, Bethesda, MD, USA). Conjunctival hyperemia was quantified by a second clinician (AR) using two digital indices, namely RRI<sup>12</sup> and EF. Both the RRI and EF indices are described by adimensional numbers ranging from 0 to 1. (See Supplementary Fig. S1 for key passages to digitally quantify conjunctival hyperemia.) The maximum amount of bulbar conjunctiva was included in the analyses, excluding everything but conjunctiva itself, such as cornea, eyelids, or eyelashes. For that purpose, a region of interest (ROI) was drawn using freehand selection around the exposed conjunctiva, and all but the ROI was replaced by a pure white background by using the “clear outside” function. Two different algorithms were applied to the resulting image in order to calculate RRI and EF.

### Software Algorithms

Relative redness of image was calculated as described by Papis<sup>12</sup> and divided by the total number of pixels, specifically:

$$RRI = \frac{\sum_{i=1} \sum_{j=1} \left( \frac{R_{ij}}{R_{ij} + G_{ij} + B_{ij}} \right)}{NoP}, \quad (1)$$

where  $i$  and  $j$  are pixel coordinates;  $R_{ij}$ ,  $G_{ij}$ , and  $B_{ij}$  are red, green, and blue intensities, respectively, for a pixel at positions  $i$  and  $j$  in the image array; and  $NoP$  is the total number of image pixels. In order to calculate RRI index, we wrote an ImageJ macro to (1) exclude pure white background (RGB code 255.255.255); (2) exclude pixels with specular reflection, defined by R, G, and B values above 220 (Ref. 10); (3) to extract R, G, and B values for each pixel; and (4) to calculate RRI.

As described by Fieguth and Simpson,<sup>11</sup> EF was calculated as the ratio between the number of edge pixels, computed by Canny edge detection algorithm,<sup>18</sup> and the total number of conjunctival pixels.

$$EF = \frac{\sum_{i \in NoP} [Canny(NoP)]_i}{NoP} \quad (2)$$

To calculate EF: (1) ImageJ function “Find edges” was launched; (2) pictures were split into the three color channels; (3) the green channel was selected because it provided the

best signal-to-noise ratio (SNR); (4) “canny edge detector” plugin (provided in the public domain by <http://rsbweb.nih.gov/ij/plugins/canny/index.html>) was launched, and plugin function “Conn Thresholding” was selected; (5) a threshold value was manually defined for every picture; (6) plugin function “Hysteresis” was used in order to get binary black and white pictures, where edge pixels were the white ones, whereas black pixels were nonedge plus background ones; (7) in order to exclude background from the computation, images were manually cut and pasted into a pure blue background (RGB code 000.000.255); and (8) an ImageJ macro was written to exclude background pixels and to calculate the number of edge, nonedge, and the edge-to-total pixels ratio.

### Sample Collection for Flow Cytometry

To avoid any interference in flow cytometric analysis, sample collection was performed prior to fluorescein application. Superficial conjunctival cells were collected through impression cytology as previously described.<sup>19,20</sup> Briefly, 1 drop oxybuprocaine hydrochloride 0.4% was instilled in patients' eyes; after 10 seconds, sterile nitrocellulose membranes (Merck Millipore Ltd., Etobicoke, ON, Canada), previously divided into two specular semicircles, were gently applied on both side of the filter to each eye onto the unexposed bulbar conjunctiva, superotemporally, inferotemporally, superonasally, and inferonasally for approximately 20 seconds. Filters were then immediately placed in 15 mL sterile tubes containing 5 mL complete medium (RPMI medium plus 10% fetal bovine serum) and kept at 4°C. Then, samples were moved into a thermic bag, carried to the Flow Cytometry Core Facility and processed within 24 hours.

### Flow Cytometry Analysis

Briefly, tubes were vortexed for 30 seconds, and filter disks were removed using a sterile forceps. Then, cells were pelleted by centrifugation for 5 minutes at 300g. Supernatant was discarded, and 50 µL dilution mixture (PBS with 1% bovine serum albumin) containing Syto-16 (final concentration 2.5 µM; Life Technologies, Monza, Italy) and monoclonal antibodies were added to the pellet for 20 minutes at room temperature. Antibodies included CD45-phycoerythrin-cyanine 7 (PE-Cy7), HLA-DR-allophycocyanin (APC), and CD14-electron coupled dye (ECD) (all Beckman Coulter, Milan, Italy), whereas CD16-APC-H7 and CD3-Pacific Blue were from Becton-Dickinson (Milan, Italy). CD15 Alexa-Fluor 700 (Campoverde, Milan, Italy) was kindly donated by G Oliveira (San Raffaele Scientific Institute, Milan, Italy). All antibodies were

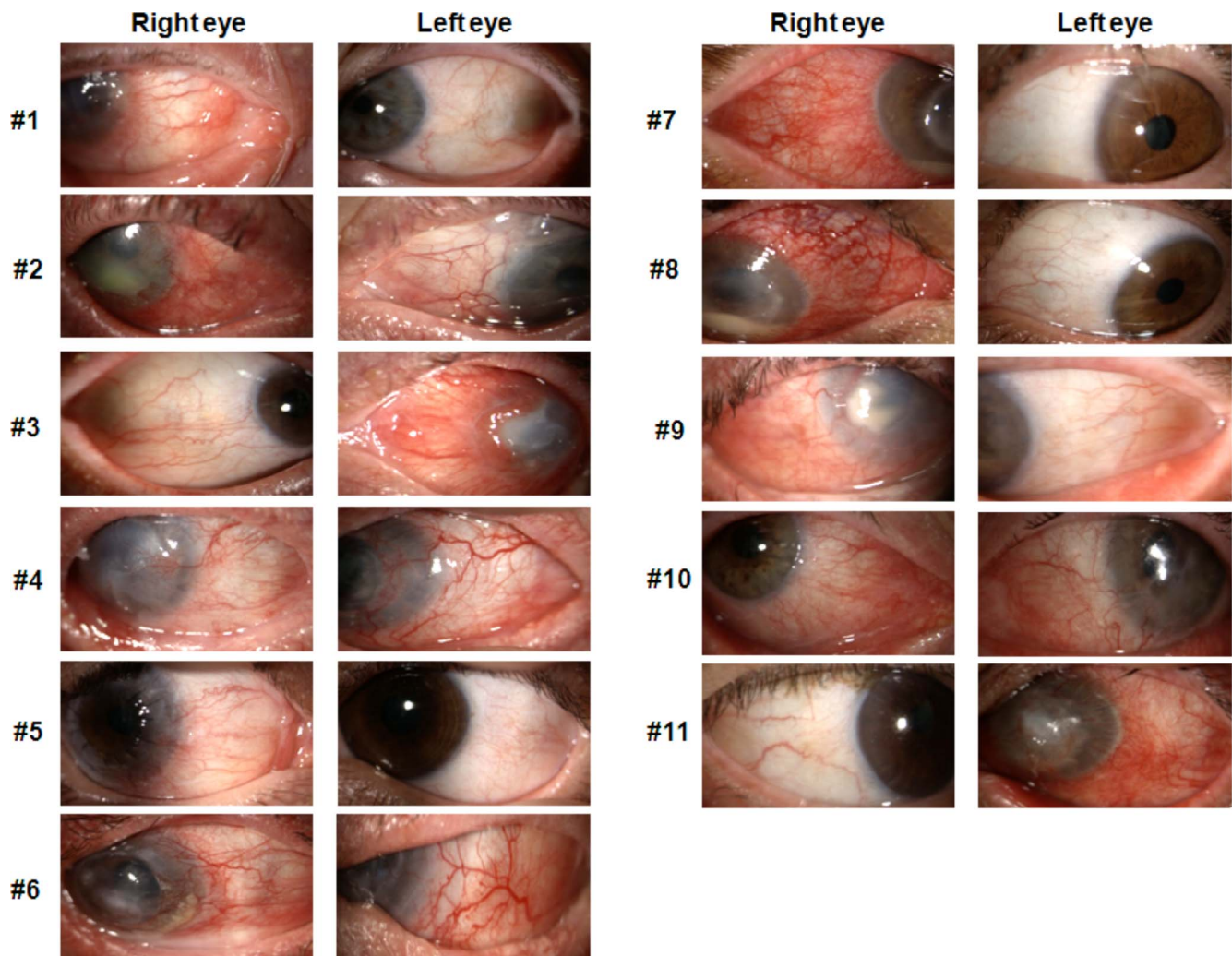


FIGURE 1. Baseline clinical views (magnification  $\times 10$ ) of eyes included in the study. Unaffected eyes were #1 left, #3 right, #7 left, #8 left, and #11 right.

properly titrated using blood samples in order to reduce background in the multicolor environment. At the end of incubation, 150  $\mu\text{L}$  PBS and propidium iodide (PI; 0.5  $\mu\text{g}/\text{mL}$  final concentration; Sigma-Aldrich, Milan, Italy) were added. Samples were acquired using a LSR Fortessa cell analyzer equipped with 355-, 405-, 488-, 561-, and 640-nm laser lines (Becton Dickinson). To check instrument performance, in order to ensure robustness and reproducibility of the data, calibrator beads (8-peaks rainbow beads; Spherotech, Lake Forest, IL, USA) were used at the beginning of each experimental session. Gating strategy was based on the exclusion of dead cells (positive for PI and Syto-16,  $\text{PI}^{\text{pos}}/\text{Syto16}^{\text{pos}}$ ) and debris (positive or negative for PI and negative for Syto16,  $\text{PI}^{\text{pos-neg}}/\text{Syto16}^{\text{neg}}$ ) from the analysis. After gating for doublet exclusion ("Singlet" gate), we characterized cells as  $\text{CD45}^{\text{dim}}$  or  $\text{CD45}^{\text{bright}}$  on the basis of fluorescence intensity of CD45 staining as observed during flow cytometry.  $\text{CD45}^{\text{dim}}$  defines the whole granulocyte population as being  $\text{CD14}^{\text{dim/neg}}$  and  $\text{CD16}^{\text{pos}}$  and  $\text{CD15}^{\text{pos}}$  as well.  $\text{CD45}^{\text{bright}}$  included lymphocytes ( $\text{CD3}^{\text{posHLA-DR}^{\text{pos/neg}}}$ ) and monocytes/macrophages, defined as  $\text{CD3}^{\text{neg}}$ ,  $\text{CD14}^{\text{bright}}$ , or  $\text{CD16}^{\text{pos}}$  (see Supplementary Fig. S2 for the visualization of gating strategy). All data were stored in a list mode file (Flow Cytometry Standard version 3.1) and were analyzed using FCS Express 4 software (DeNovo Software, Glendale, CA, USA). Data were

expressed as the percentage of the population of interest in the parental gate (i.e.,  $\% \text{CD45}^{\text{dim}}$  in the "Singlet" gate).

### Statistical Analysis

All data were expressed as means  $\pm$  standard error of the mean (SEM). All measurements (first and second visits) were pooled. Differences between affected and unaffected eyes were assessed using *t*-test and Mann-Whitney *U* test for parametric and nonparametric variables, respectively. Relationship between variables was investigated using Spearman correlation tests. A *P* value less than 0.05 was considered significant. Prism 5.0 software (GraphPad Software, San Diego, CA, USA) was used to analyze the data.

## RESULTS

### Clinical Data

Patients' eyes at D0 examination are shown in Figure 1. Ocular signs and conjunctival hyperemia grading scores in affected and unaffected eyes are shown in Figure 2. Visual analogue score questionnaire scores (Fig. 2A) were  $33.47 \pm 3.60$  and  $3.54 \pm 3.22$  in affected and unaffected eyes, respectively ( $P < 0.0001$ ). NEI-VFQ 25 score was  $40.37 \pm 4.58$  (data not shown).

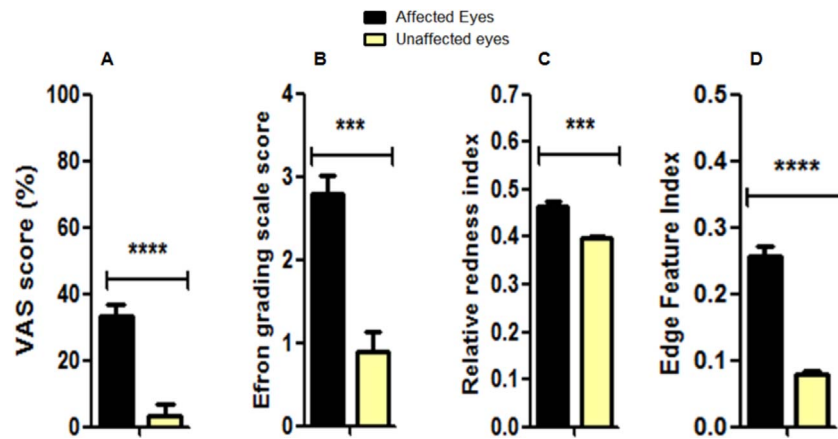


FIGURE 2. Statistical comparison of VAS (A), Efron scale for conjunctival redness (B), RRI (C), and EF (D) scores between affected ( $n = 31$ ) and unaffected eyes ( $n = 9$ ). Mann-Whitney  $U$  test was used to assess differences between the two groups for factors (B–D), whereas unpaired  $t$ -test was used for (A). \*\*\*Significant at  $P < 0.001$ ; \*\*\*\*Significant at  $P < 0.0001$ ; error bars indicate SEM.

Conjunctival hyperemia assessed with both clinical and digital score systems was significantly greater in affected eyes than in unaffected ones. Specifically, Efron scores for conjunctival hyperemia (Fig. 2B) were  $2.79 \pm 0.23$  and  $0.90 \pm 0.23$  in affected and unaffected eyes, respectively ( $P = 0.0003$ ). With regard to digital scores, RRIs (Fig. 2C) were  $0.46 \pm 0.01$  and  $0.40 \pm 0.01$  in affected and unaffected eyes, respectively ( $P = 0.0004$ ); and EFs (Fig. 2D) were  $0.25 \pm 0.02$  and  $0.08 \pm 0.01$ , respectively ( $P < 0.0001$ ). As shown in Figure 3, Efron score strongly correlated with both RRI (Spearman  $r = 0.93$ ,  $P < 0.0001$ ) and EF (Spearman  $r = 0.81$ ,  $P < 0.0001$ ). Edge feature and RRI correlated with each other (Spearman  $r = 0.78$ ,  $P < 0.0001$ ) (Fig. 3C). NEI-VFQ25 negatively correlated with patients' worst VAS scores (Spearman  $r = -0.52$ ,  $P = 0.0195$ ) (data not shown). No further correlations were appreciated between NEI-VFQ 25 and VAS, RRI, or EF (data not shown). Finally, no significant differences were found between D0 and D1 in any of the parameters considered.

### Flow Cytometry Results

Baseline impression cytology data of one affected eye (patient 9, right eye) were excluded from analysis due to insufficient sample retrieval. Supplementary Figure S2 shows gating strategies used to determine cellular populations. CD45<sup>bright</sup> and CD45<sup>dim</sup> leukocyte percentages were significantly different between the two groups. Specifically, CD45<sup>dim</sup> cells were

$51.10\% \pm 6.84\%$  and  $18.62\% \pm 10.09\%$  ( $P = 0.0080$ ), whereas CD45<sup>bright</sup> leucocytes were  $37.05\% \pm 6.03\%$  and  $72.45\% \pm 9.78\%$  ( $P = 0.0054$ ) in affected and unaffected eyes, respectively. No significant differences between the two groups were appreciated in CD45<sup>bright</sup>CD3<sup>pos</sup> T lymphocytes ( $P = 0.3084$ ), CD45<sup>bright</sup>CD3<sup>neg</sup> cells ( $P = 0.2492$ ), activated CD45<sup>bright</sup>CD3<sup>pos</sup>HLA-DR<sup>pos</sup> T lymphocytes ( $P = 0.4481$ ), CD45<sup>bright</sup>CD3<sup>neg</sup>HLA-DR<sup>pos</sup> cells ( $P = 0.6980$ ), or CD45<sup>bright</sup>CD3<sup>neg</sup>CD14<sup>bright</sup>, CD16<sup>pos</sup> monocytes ( $P = 0.3525$ ). Flow cytometry results, expressed as percentages, in affected and unaffected eyes are shown in Figure 4.

### Correlation Analysis

VAS and digital hyperemia grading systems were significantly correlated (Fig. 5). Specifically, a positive correlation was appreciated between ocular symptoms and conjunctival hyperemia, namely between VAS score and both RRI (Spearman  $r = 0.53$ ,  $P = 0.0004$ ) and EF (Spearman  $r = 0.62$ ,  $P < 0.0001$ ) (Figs. 5A, 5B). Moreover, ocular symptoms correlated directly with the presence of CD45<sup>dim</sup> granulocytes (Spearman  $r = 0.46$ ,  $P = 0.0031$ ) (Fig. 5C) and inversely with CD45<sup>bright</sup> cells (Spearman  $r = -0.35$ ,  $P = 0.0298$ ) (Fig. 5D). None of the other flow cytometry markers were correlated with VAS score. Figures 6 and 7 show correlation between conjunctival hyperemia, expressed as RRI and EF scores, and flow cytometry markers. The granulocyte infiltrate (Figs. 6A, 6B)

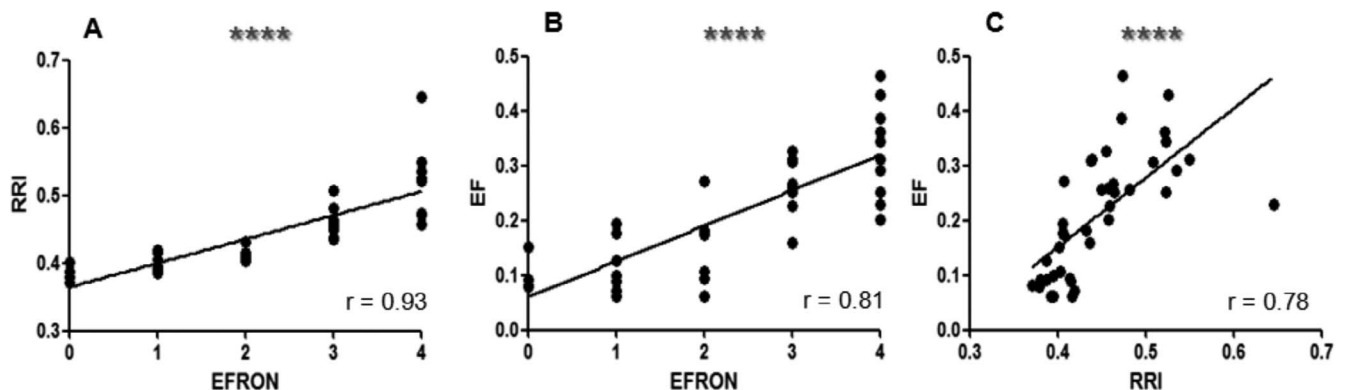
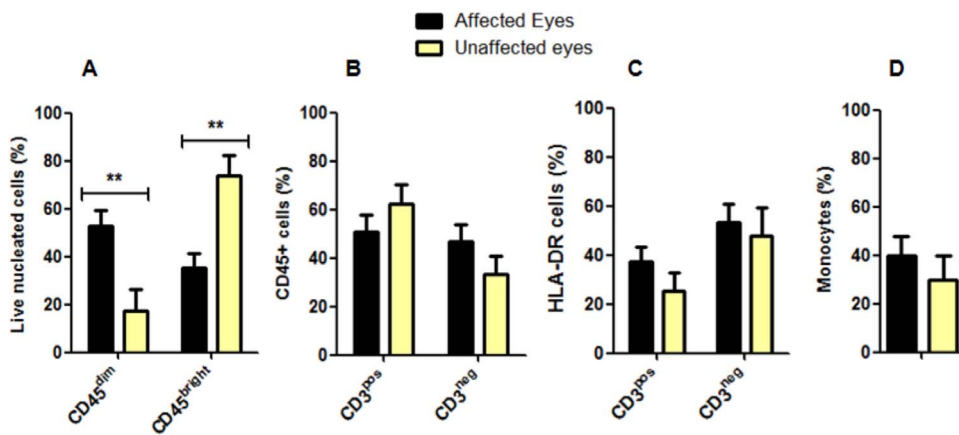


FIGURE 3. The digital parameters relative redness index and edge features were positively correlated with the Efron scale (A, B) and to each other (C). Number of samples = 40; \*\*\*\*Significant at  $P < 0.0001$ ;  $r$  = Spearman's rank correlation coefficient.



**FIGURE 4.** Impression cytology cell populations are different between inflamed ( $n = 30$ ) and noninflamed ( $n = 9$ ) eyes. Statistical comparison of CD45<sup>dim</sup> and CD45<sup>bright</sup> leukocytes (A), CD45<sup>bright</sup>CD3<sup>pos</sup> and CD45<sup>bright</sup>CD3<sup>neg</sup> cells (B), activated T and non-T cells defined as HLA-DR<sup>pos</sup> cells (C), and monocytes (D). Mann-Whitney  $U$  test was used to assess differences between the two groups. \*\*Significant at  $P < 0.01$ ; error bars indicate SEM.

correlated directly with both RRI (Spearman  $r = 0.69$ ,  $P < 0.0001$ ) and EF (Spearman  $r = 0.64$ ,  $P < 0.0001$ ), whereas total conjunctival CD45<sup>bright</sup> leukocytes were inversely related with RRI (Spearman  $r = -0.57$ ,  $P = 0.0002$ ) (Fig. 6C) and EF (Spearman  $r = -0.58$ ,  $P < 0.0001$ ) (Fig. 6D). Among CD45<sup>bright</sup> leukocytes, T lymphocytes were inversely correlated with RRI (Spearman  $r = -0.41$ ,  $P = 0.0105$ ) and EF (Spearman  $r = -0.43$ ,  $P = 0.0064$ ) (Figs. 7A, 7B), while CD45<sup>bright</sup>CD3<sup>neg</sup> cells directly correlated with RRI (Spearman  $r = 0.39$ ,  $P = 0.0147$ ) (Fig. 7C) and EF (Spearman  $r = 0.42$ ,  $P = 0.0075$ ) (Fig. 7D). The

remaining cell populations were not significantly correlated to RRI or EF. No correlation was appreciated between NEI-VFQ 25 and any cell population (data not shown).

## DISCUSSION

In this paper, we report a semiautomatic method to objectively quantify ocular hyperemia using instruments commonly found in every ophthalmic outpatient clinic (i.e., a slit-lamp unit and a

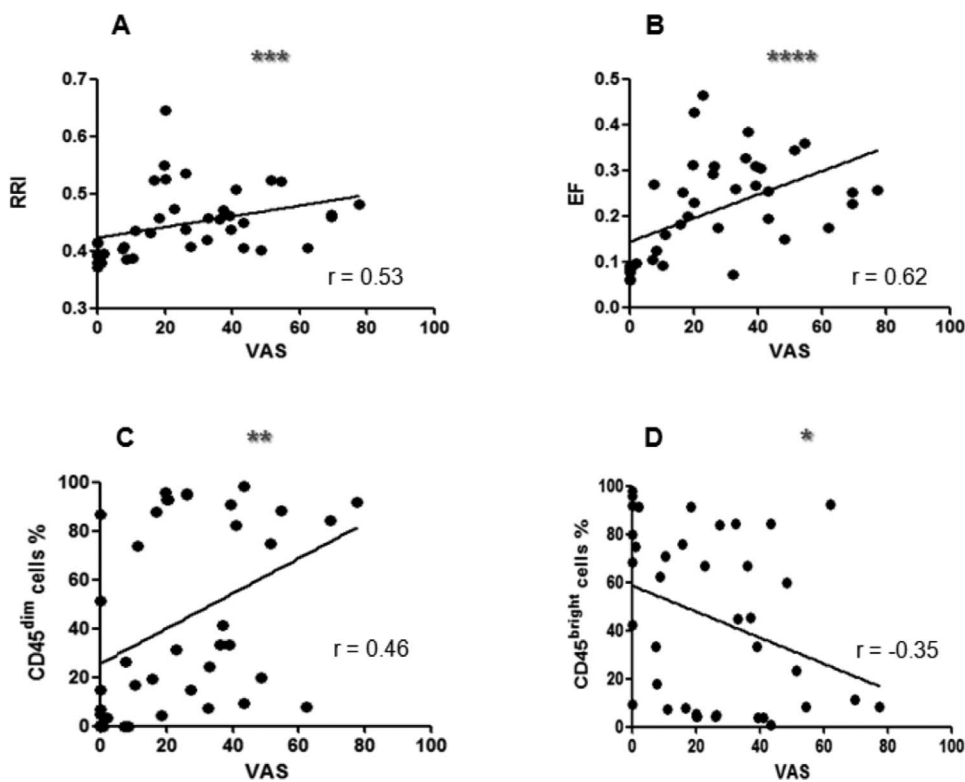


**FIGURE 5.** Relative redness index and edge features and CD45<sup>dim</sup> and CD45<sup>bright</sup> cells are directly correlated with visual analogue scale. Correlation between (A) VAS and RRI, (B) VAS and EF (C) VAS and granulocytes, and (D) VAS and CD45<sup>bright</sup> cells. Number of samples = 39; \*significant at  $P < 0.05$ ; \*\*significant at  $P < 0.01$ ; \*\*\*significant at  $P < 0.001$ ; \*\*\*\*significant at  $P < 0.0001$ ;  $r$  = Spearman's rank correlation coefficient.

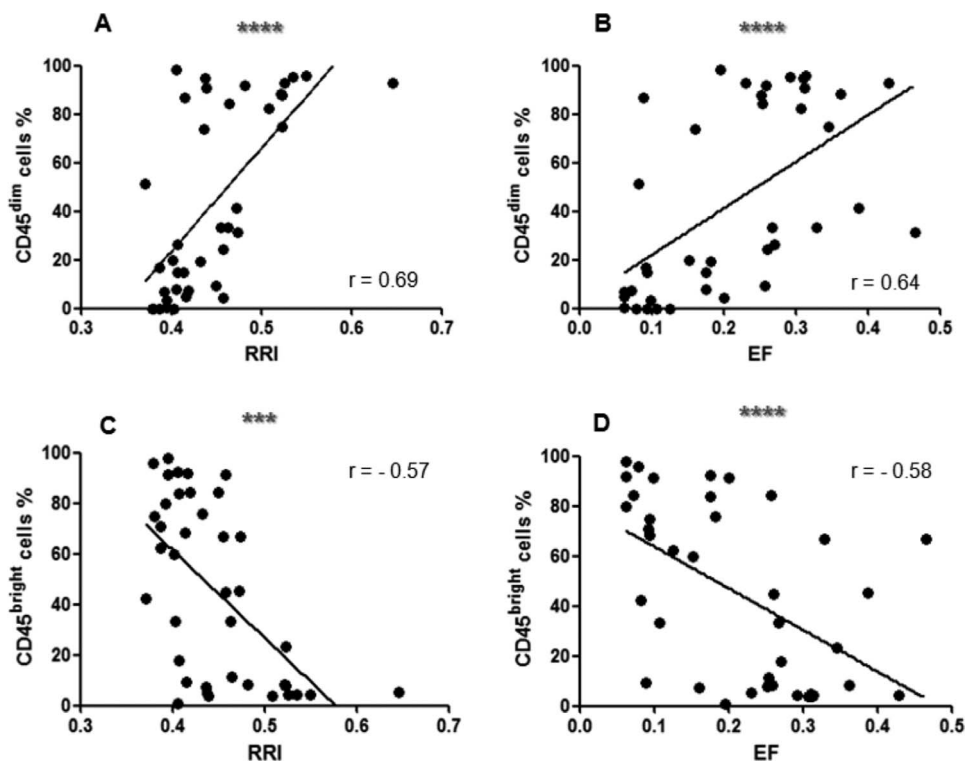


FIGURE 6. CD45<sup>dim</sup> and CD45<sup>bright</sup> cells are correlated with RRI and EF. Correlation between (A) RRI and granulocytes, (B) EF and granulocytes, (C) RRI and CD45<sup>bright</sup> cells, and (D) EF and CD45<sup>bright</sup> cells. Number of samples = 39; \*\*\*significant at  $P < 0.001$ ; \*\*\*\* significant at  $P < 0.0001$ ;  $r$  = Spearman's rank correlation coefficient.

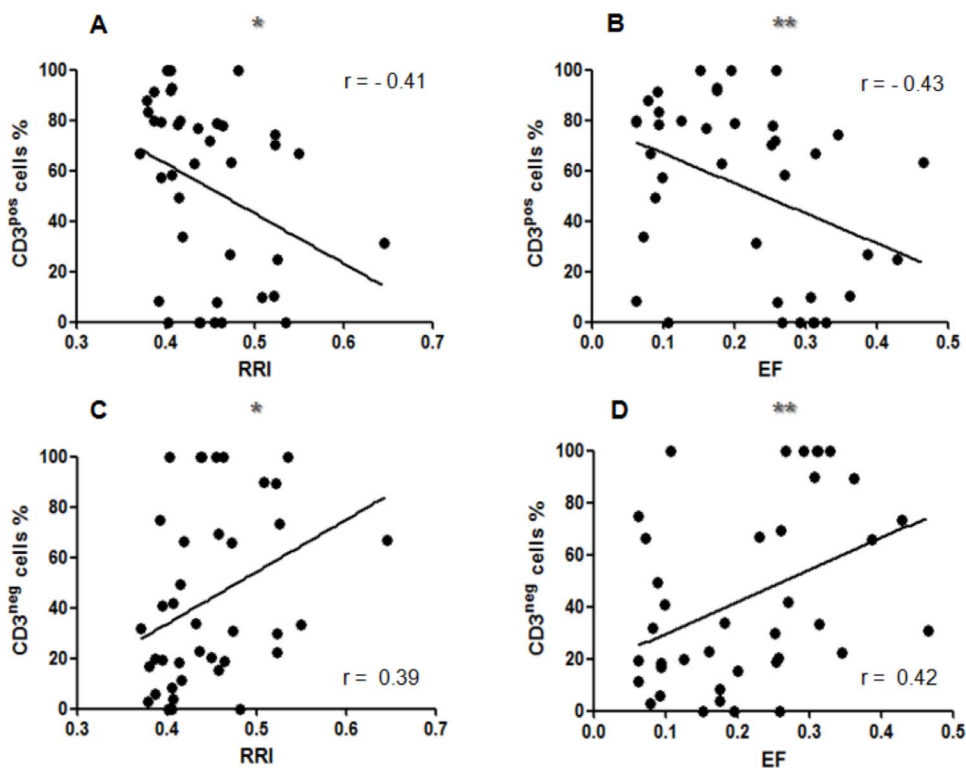


FIGURE 7. CD45<sup>bright</sup>CD3<sup>pos</sup> and CD45<sup>bright</sup>CD3<sup>neg</sup> correlated to RRI and EF. Correlation between (A) RRI and T cells, (B) EF and T cells, (C) RRI and CD45<sup>bright</sup>CD3<sup>neg</sup> cells, and (D) EF and CD45<sup>bright</sup>CD3<sup>neg</sup> cells. Number of samples = 39; \*significant at  $P < 0.05$ ; \*\*significant at  $P < 0.01$ ;  $r$  = Spearman's rank correlation coefficient.

computer) in a simple and low-cost way. Among all proposed strategies to quantify conjunctival redness, edge detection (i.e., EF) and relative color extraction (i.e., RRI) appeared to be the most stable, reliable, and sensitive; moreover, such techniques were highly correlated with clinical grading scales.<sup>21</sup> Peterson et al.<sup>21</sup> proposed that edge detection and relative color extraction resemble the clinical perception of conjunctival hyperemia, which mostly relies on vessels coverage area and ocular redness, in a more objective and reliable way.

Furthermore, to increase the correlation with robust and well-described biological markers of ocular surface inflammation, we evaluated the amount and phenotype of conjunctival inflammatory cell infiltration by means of impression cytology and flow cytometry. Our results confirm a solid increase in granulocytes in inflamed eyes, as reported by Williams et al.,<sup>22</sup> although CD45<sup>bright</sup> cells were significantly reduced. The percentages of monocytes and T lymphocytes were not significantly different between the two groups, although monocytes were most represented in inflamed eyes and T lymphocytes in noninflamed eyes. Because flow cytometry data are expressed as percentages, CD45<sup>bright</sup> cells were probably reduced in inflamed eyes due to the concomitant increase of CD45<sup>dim</sup> granulocytes. Additionally, it is well known that granulocytes are more represented than lymphocytes and monocytes in acute corneal inflammation, which affected the patients recruited in this study, and that they play a crucial role in pathogen elimination and resolution of inflammation.<sup>23</sup>

In order to test whether our findings might have relevance in a clinical setting, such as a clinical trial, we searched for correlations between clinical redness indices and infiltrating inflammatory cells. Interestingly, ocular redness was positively correlated with granulocytes and CD45<sup>bright</sup>CD3<sup>neg</sup> non-T cells, whereas total CD45<sup>bright</sup> cells and CD45<sup>bright</sup>CD3<sup>pos</sup> T lymphocytes exhibited a negative correlation. The CD45<sup>bright</sup>CD3<sup>neg</sup> population contains monocytes that, despite the absence of significant correlation, are increased in affected eyes and could play a role in active inflammation, together with other CD3<sup>neg</sup> cells such as NK cells. Indeed, the presence of NK cells was instrumental to the development of maximal ocular surface inflammation.<sup>24</sup> On the other hand, we found that the percentage of T lymphocytes was inversely related to ocular redness indices. This could be due to the presence of regulatory T cells, which are known for their immunomodulatory activity. In fact, this specific lymphocyte subset has been associated with reduction of inflammation.<sup>25</sup> Such correlations between ocular redness and cytofluorimetric markers was statistically significant also when the Efron scale was used. We further analyzed our data, creating homogenous diagnostic groups, specifically, ocular cicatricial pemphigoid and bacterial ulcer. Cicatricial pemphigoid patients (two patients with both eyes affected) showed higher percentages of CD45<sup>dim</sup> cells than CD45<sup>bright</sup> cells (cumulative results for the median of the two eyes at two time points: CD45<sup>dim</sup>: 85.12% versus those in CD45<sup>bright</sup>: 6.17%). Interestingly, the majority of CD45<sup>bright</sup> cells were CD3<sup>neg</sup> (cumulative results for the median of the two eyes at the two time points: CD3<sup>neg</sup>: 95% vs. CD3<sup>pos</sup>: 5%). Thus, a small population of CD3<sup>pos</sup> cells is present in the conjunctiva of pemphigoid patients. Indeed, T lymphocytes have a significant role in the disease, as described before.<sup>26</sup> In the two patients suffering from corneal bacterial ulcers we noticed a prevalence of CD45<sup>dim</sup> at the first time point in the affected eye (patient 9: 95.59%; patient 11: 88.09%), whereas at the second time point the percentage of CD45<sup>dim</sup> decreased for patient 9 to 31.53% (patient 11 was lost to follow-up), whereas CD3<sup>pos</sup> cells increased to 66.67%. Although the

limited sample does not allow a definitive conclusion, this could reflect a switch in the immune response toward a Th1/Th2 phenotype (extensively studied in mouse models by Hazlett and Hendricks<sup>27</sup>) after an infiltration of polymorphonucleated cells in a very early phase of the infection. Indeed, the presence of lymphocytes has been described in viral, but also bacterial keratitis.<sup>28</sup> The Th1/Th2 switch could explain the weaker correlation between CD3 and redness indexes. In fact, these cells could actively stimulate inflammation or, on the contrary, play a role in immune modulation. Further studies are needed to address additional phenotypic characterization, to better dissect the role of T lymphocyte subpopulations and other non-T-cell subsets (monocytes, NK cells) in the setting of conjunctival hyperemia.

A potential limitation of our grading, which is shared by all other computerized methods, is the time required to process images, which is greater than that needed to complete clinical grading scales. We estimated that in this study, the time needed to take the eye pictures and to analyze them with both RRI and EF was approximately 5 minutes. We think that time can be reduced when the operator gains experience, and is short enough to keep the procedure feasible. Another potential limitation is represented by some source of residual variability, in particular regarding image acquisition at the slit-lamp; conjunctival ROI selection; and choice of threshold values for EF (not for RRI). Many studies, including ours, have tried to minimize variability in image acquisition by setting fixed slit-lamp parameters.<sup>10,11,13</sup> In addition, Amparo et al.<sup>10</sup> proposed an elegant white-balance correction algorithm to balance differences in lightening conditions. With regard to conjunctival ROIs selection, small interoperator differences should be unimportant given the large amount of total conjunctiva and the fact that the indices do not depend on the number of pixels.

In summary, we report a novel, semiautomated method to quantify ocular surface inflammation. This quantification requires a slit-lamp and a personal computer, which are generally available in any clinical setting. Two indices are generated as an output, and they are significantly correlated with the percentages of CD45<sup>dim</sup>granulocytes, total CD45<sup>bright</sup> cells, CD45<sup>bright</sup>CD3<sup>pos</sup> T lymphocytes and CD45<sup>bright</sup>CD3<sup>neg</sup> non-T cells. Because conjunctival redness is a key sign of inflammation and significantly drives clinical judgment in highly prevalent ocular disorders, we suggest that this method may represent a useful tool in the follow-up of these disorders. Additionally, it could be used as a robust endpoint measure in clinical trials testing anti-inflammatory treatments of the ocular surface.

### Acknowledgments

Disclosure: **G. Ferrari**, None; **A. Rabiolo**, None; **F. Bignami**, None; **F. Sizzano**, None; **A. Palini**, None; **C. Villa**, None; **P. Rama**, None

### References

1. Rowe AM, St Leger AJ, Jeon S, Dhaliwal DK, Knickelbein JE, Hendricks RL. Herpes keratitis. *Prog Retin Eye Res.* 2013;32:88-101.
2. Chang JH, Wakefield D. Uveitis: a global perspective. *Ocul Immunol Inflamm.* 2002;10:263-279.
3. Hessen M, Akpek EK. Dry eye: an inflammatory ocular disease. *J Ophthalmic Vis Res.* 2014;9:240-250.
4. Leibowitz HM. The red eye. *N Engl J Med.* 2000;343:345-351.
5. Efron N. Grading scales for contact lens complications. *Ophthalmic Physiol Opt.* 1998;18:182-186.

6. Schulze MM, Jones DA, Simpson TL. The development of validated bulbar redness grading scales. *Optom Vis Sci.* 2007;84:976-983.
7. McMonnies CW, Chapman-Davies A. Assessment of conjunctival hyperemia in contact lens wearers. Part II. *Am J Optom Physiol Opt.* 1987;64:251-255.
8. Terry RSD, Wong R, Papas E. Variability of clinical investigators in contact lens research. *Optom Vis Sci.* 1995;72:16.
9. Chong TST, Fonn D. The repeatability of discrete and continuous anterior segment grading scales. *Optom Vis Sci.* 2000;77:244-251.
10. Amparo F, Wang H, Emami-Naeini P, Karimian P, Dana R. The ocular redness index: a novel automated method for measuring ocular injection. *Invest Ophthalmol Vis Sci.* 2013;54:4821-4826.
11. Fieguth P, Simpson T. Automated measurement of bulbar redness. *Invest Ophthalmol Vis Sci.* 2002;43:340-347.
12. Papas EB. Key factors in the subjective and objective assessment of conjunctival erythema. *Invest Ophthalmol Vis Sci.* 2000;41:687-691.
13. Rodriguez JD, Johnston PR, Ousler GW III, Smith LM, Abelson MB. Automated grading system for evaluation of ocular redness associated with dry eye. *Clin Ophthalmol.* 2013;7:1197-1204.
14. Schulze MM, Hutchings N, Simpson TL. The use of fractal analysis and photometry to estimate the accuracy of bulbar redness grading scales. *Invest Ophthalmol Vis Sci.* 2008;49:1398-1406.
15. Ohashi Y, Ebihara N, Fujishima H, et al. A randomized, placebo-controlled clinical trial of tacrolimus ophthalmic suspension 0.1% in severe allergic conjunctivitis. *J Ocul Pharmacol Ther.* 2010;26:165-174.
16. Mangione CM, Lee PP, Gutierrez PR, et al. Development of the 25-item National Eye Institute Visual Function Questionnaire. *Arch Ophthalmol.* 2001;119:1050-1058.
17. Rossi GC, Milano G, Tinelli C. The Italian version of the 25-item National Eye Institute Visual Function Questionnaire: translation, validity, and reliability. *J Glaucoma.* 2003;12:213-220.
18. Canny J. A computational approach to edge detection. *IEEE Trans Comput.* 1986;6:679-698.
19. Brignole-Baudouin F, Ott AC, Warnet JM, Baudouin C. Flow cytometry in conjunctival impression cytology: a new tool for exploring ocular surface pathologies. *Exp Eye Res.* 2004;78:473-481.
20. Epstein SP, Gadaria-Rathod N, Wei Y, Maguire MG, Asbell PA. HLA-DR expression as a biomarker of inflammation for multicenter clinical trials of ocular surface disease. *Exp Eye Res.* 2013;111:95-104.
21. Peterson RC, Wolffsohn JS. Objective grading of the anterior eye. *Opt Vis Sci.* 2009;86:273-278.
22. Williams GP, Tomlins PJ, Denniston AK, et al. Elevation of conjunctival epithelial CD45INTCD11b(+)CD16(+)/CD14(-) neutrophils in ocular Stevens-Johnson syndrome and toxic epidermal necrolysis. *Invest Ophthalmol Vis Sci.* 2013;54:4578-4585.
23. Kolaczowska E, Kubes P. Neutrophil recruitment and function in health and inflammation. *Nat Rev Immunol.* 2013;13:159-175.
24. Reyes NJ, Mayhew E, Chen PW, Niederkorn JY. NKT cells are necessary for maximal expression of allergic conjunctivitis. *Int Immunol.* 2010;22:627-636.
25. Sehrawat S, Suvas S, Sarangi PP, Suryawanshi A, Rouse BT. In vitro-generated antigen-specific CD4+ CD25+ Foxp3+ regulatory T cells control the severity of herpes simplex virus-induced ocular immunoinflammatory lesions. *J Virol.* 2008;82:6838-6851.
26. Elder MJ, Lightman S. The immunological features and pathophysiology of ocular cicatricial pemphigoid. *Eye (Lond).* 1994;8(pt 2):196-199.
27. Hazlett LD, Hendricks RL. Reviews for immune privilege in the year 2010: immune privilege and infection. *Ocul Immunol Inflamm.* 2010;18:237-243.
28. Kwon B, Hazlett LD. Association of CD4+ T cell-dependent keratitis with genetic susceptibility to *Pseudomonas aeruginosa* ocular infection. *J Immunol.* 1997;159:6283-6290.